



Airborne virus collection using the BioSampler at various sampling flow rates and periods under different airborne virus concentrations and collection liquid volumes

Chaewoon Jung, Wonyoung Jeon, Vidhurathan Soundararajan & Jaesung Jang

To cite this article: Chaewoon Jung, Wonyoung Jeon, Vidhurathan Soundararajan & Jaesung Jang (2026) Airborne virus collection using the BioSampler at various sampling flow rates and periods under different airborne virus concentrations and collection liquid volumes, *Aerosol Science and Technology*, 60:3, 277-291, DOI: [10.1080/02786826.2025.2591217](https://doi.org/10.1080/02786826.2025.2591217)

To link to this article: <https://doi.org/10.1080/02786826.2025.2591217>



© 2025 The Author(s). Published with license by Taylor & Francis Group, LLC.



[View supplementary material](#)



Published online: 05 Dec 2025.



[Submit your article to this journal](#)



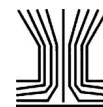
Article views: 461



[View related articles](#)



[View Crossmark data](#)



Airborne virus collection using the BioSampler at various sampling flow rates and periods under different airborne virus concentrations and collection liquid volumes

Chaewoon Jung^a, Wonyoung Jeon^a, Vidhurathan Soundararajan^a, and Jaesung Jang^{a,b,c}

^aDepartment of Mechanical Engineering, Ulsan National Institute of Science and Technology (UNIST), Ulsan, Republic of Korea;

^bDepartment of Biomedical Engineering, UNIST, Ulsan, Republic of Korea; ^cDepartment of Civil, Urban, Earth, and Environmental Engineering, UNIST, Ulsan, Republic of Korea

ABSTRACT

The SKC BioSampler has been widely utilized as a standard microbial air sampler, and its manufacturer recommends a sampling flow rate of 12.5 L/min. However, the effects of sampling flow rates on the collection of airborne viruses have rarely been studied. In this study, we assessed the collection of airborne MS2 viruses using the SKC BioSampler at various sampling flow rates (4.0, 8.0, 10.0, 12.5, and 13.3 [±0.01] Standard L/min (SLPM); standard conditions: 21.1 °C and 101.3 kPa), sampling periods (10, 60, and 360 min), and airborne virus concentrations (10^8 , 10^6 , and 10^4 PFU/m³) in 20-mL collection liquid. The concentrations of infectious viruses in the collected samples and collection efficiencies for MS2 viruses increased with the sampling flow rate at 10- and 60-min sampling periods, except at the lowest airborne virus concentration. Moreover, a sampling flow rate of 13.3 SLPM was the most efficient for collecting airborne viable MS2 viruses. At $\sim 10^4$ PFU/m³ of air, close to the field-level concentrations of respiratory viruses, viable MS2 viruses were detected at 10.0–13.3 SLPM during 360-min sampling. The gene copy concentrations and collection efficiencies for influenza viruses were also measured using RT-qPCR at various sampling flow rates (10.0–13.3 SLPM), and at two concentrations (10^6 and 10^5 gene copies/m³ of air) and collection liquid volumes (20 mL and 13 mL). Similar to MS2 viruses, 13.3 SLPM was the most efficient for collecting the nucleic acids of influenza viruses.

ARTICLE HISTORY

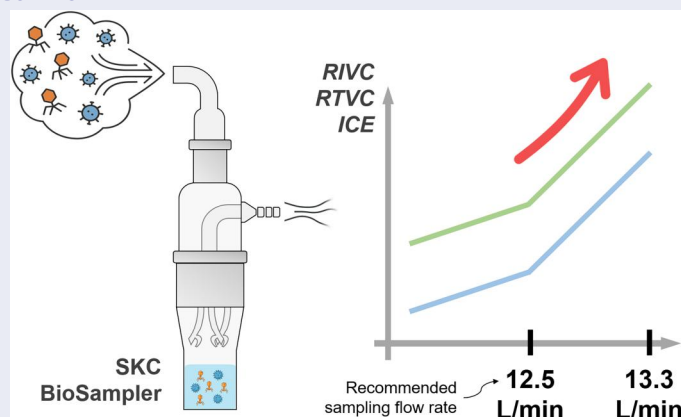
Received 22 April 2025

Accepted 7 November 2025

EDITOR

Shanna Ratnesar-Shumate

GRAPHICAL ABSTRACT



CONTACT Jaesung Jang ✉ jjang@unist.ac.kr 📧 Department of Mechanical Engineering, Ulsan National Institute of Science and Technology (UNIST), Ulsan 44919, Republic of Korea.

📄 Supplemental data for this article can be accessed online at <https://doi.org/10.1080/02786826.2025.2591217>.

© 2025 The Author(s). Published with license by Taylor & Francis Group, LLC.

This is an Open Access article distributed under the terms of the Creative Commons Attribution-NonCommercial-NoDerivatives License (<http://creativecommons.org/licenses/by-nc-nd/4.0/>), which permits non-commercial re-use, distribution, and reproduction in any medium, provided the original work is properly cited, and is not altered, transformed, or built upon in any way. The terms on which this article has been published allow the posting of the Accepted Manuscript in a repository by the author(s) or with their consent.

1. Introduction

In recent several decades, respiratory viruses, such as influenza viruses and coronaviruses, have caused significant health-related problems, as observed during the COVID-19 pandemic. Respiratory viruses can infect people through various transmission routes, such as droplets, direct and indirect contact, and aerosols (Bhardwaj et al. 2021). Among these routes, aerosol transmission is particularly crucial as virus particles can remain suspended in the air for hours depending on their size and infect others rapidly through inhalation (Wang et al. 2021). Thus, measuring the concentration of respiratory viruses in the air is essential for preventing the spread of infectious diseases *via* aerosol transmission, and air sampling is the first step in this measurement.

Numerous microbial air samplers, such as filters, impactors, impingers, cyclones, and condensation and electrostatic samplers, have been developed to collect airborne virus particles (Pan et al. 2019; Bhardwaj et al. 2021). Among these samplers, the SKC BioSampler (SKC Inc., PA, USA) can collect various types of bioaerosol particles *via* swirling with simplicity and cost-effectiveness. It was reported to prevent desiccation, moderate the stress exerted on microorganisms, and reduce the bounce of collected particles, thereby preserving the viability of collected microorganisms (Willeke et al. 1998).

The SKC BioSampler has been extensively used as a separate or a reference sampler for detection of airborne viruses (Memish et al. 2014; Lednicky et al. 2016; Kenarkoohi et al. 2020; Kim et al. 2021; Jang et al. 2022; Vives et al. 2022; Lee et al. 2024) despite its relatively low collection efficiency for submicrometer-sized virus particles (Hogan et al. 2005; Li et al. 2018). It was also reported to exhibit higher virus collection efficiencies than gelatin and glass fiber filters (Fabian et al. 2009; Li et al. 2018).

Airborne virus collection using the BioSampler can be affected by several parameters, such as the sampling period, flow rate, and volume of collection liquid, in addition to the particle diameter. In most studies, the sampling periods in the lab-scale and field tests were ≤ 1 h and ≥ 1 h, respectively. The sampling flow rate was 12.5 L/min, and the volume of collection liquid was 20 mL, as recommended by the manufacturer.

Other sampling flow rates were also adopted in many studies (Table 1); however, the effect of flow rates was investigated in a few studies. Hogan et al. (2005) measured physical collection efficiencies at sampling flow rates of 3.5–14.5 L/min and reported U-shaped and almost linear collection efficiencies for 25- and 300-nm particles, respectively, using a scanning mobility particle sizer (SMPS). On the other hand, Anwar et al. (2010) reported

that sampling flow rates of 6 and 9 L/min were more efficient than a sampling flow rate of 12.5 L/min for collecting airborne viable viruses. Based on this observation, condensation-based samplers were compared with the BioSampler at sampling flow rates of 6–8 L/min in subsequent researches (Jiang et al. 2016; Lednicky et al. 2016; Pan et al. 2016, 2017). These two aforementioned studies were conducted using highly concentrated virus suspensions in a nebulizer, leading to high virus concentrations in the air. Such effects on virus collection using the BioSampler need to be studied. Moreover, the BioSampler has been used in many field tests at sampling periods of 1–3 h (Memish et al. 2014; Nguyen et al. 2017; Pan et al. 2017; Kenarkoohi et al. 2020), which is generally accompanied by a significant amount of evaporation of collection liquids and hence a change in collection efficiency during air sampling.

Herein, we assessed the collection of airborne viruses using the BioSampler at various sampling flow rates (including 12.5 L/min), sampling periods, and airborne virus concentrations at the inlet of the BioSampler. The volume of collection liquid in the BioSampler was 20 or 13 mL to examine the effect of these two collection volumes on airborne virus collection.

We measured the concentrations of MS2 and influenza viruses in the collected samples relative to their respective concentrations in nebulizer suspensions using the plaque assay and reverse transcription-quantitative polymerase chain reaction (RT-qPCR), respectively. We also measured the concentrations of these two types of airborne viruses at the inlet of the BioSampler using gelatin filters and a water condensation-based sampler, respectively, to compute the collection efficiencies for the viruses.

In this study, the sampling flow rate of the BioSampler was adjusted based on the flow rate measurement at the inlet, as recommended by the manufacturer of the BioSampler, although it was based on volumetric flow rate measurement at the outlet of the BioSampler in many studies (Hogan et al. 2005; Anwar et al. 2010; Oh et al. 2010; Woo et al. 2012; Zheng and Yao 2017). In fact, as the airflow through the nozzles of the BioSampler exhibits large pressure drops at high flow rates (~ 0.5 bar at 12.5 L/min), the discrepancy in volumetric flow measurements between the inlet and outlet becomes significant.

2. Materials and methods

2.1. Test viruses

MS2 (ATCC 15597-B1), a single-stranded RNA bacteriophage, was used in the present study due to its similarity to many pathogenic viruses, serving as a common surrogate

Table 1. Studies on the collection of airborne viruses using the BioSampler at sampling flow rates other than 12.5 L/min.

Reference	Target viruses (Conc. in the virus suspension)	Sampling periods (min)	Sampling flow rates (L/min)	Collection liquid volume (mL)	Detection methods	Remark
(Hogan et al. 2005)	· MS2 (5×10^9 PFU/mL) · T3 (2.3×10^8 PFU/mL)	· 5/10/30/60	· 3.5/6.25/12.5/14.5	· 20	· Plaque assay · SMPS	· Comparison of samplers · Lab-scale study
(Doel et al. 2009)	· Foot-and-mouth disease virus (0.5 mL of $10^{5.0}$ TCID ₅₀ inoculated to pigs)	· 5/10/20	· 11	· 20	· ELISA · PCR	· Comparison of samplers
(Anwar et al. 2010)	· MS2 (10^8 – 10^9 PFU/mL)	· 5/15/30/45/60	· 3/6/9/12.5	· 15	· TCID ₅₀ assay · Plaque assay	· Comparison of samplers · Lab-scale study · Field sampling
(Memish et al. 2014)	· Influenza B · Human Coronavirus OC-43 · Human Adenovirus	· 120	· 6	· 20	· PCR	
(Jiang et al. 2016)	· MS2 (10^8 – 10^9 PFU/mL)	· 15	· 7	· 20	· Plaque assay · PCR	· Comparison of samplers · Lab-scale study
(Pan et al. 2016)	· MS2 (10^8 – 10^9 PFU/mL)	· 5/10/15	· 8	· 20	· Plaque assay	· Comparison of samplers · Lab-scale study
(Lednicky et al. 2016)	· Influenza A H1N1 (low: 3.4×10^7 TCID ₅₀ /mL, medium: 4.64×10^6 TCID ₅₀ /mL, high: 6.31×10^7 TCID ₅₀ /mL)	· 5/10/15	· 6.86	· 15	· TCID ₅₀ assay	· Comparison of samplers · Lab-scale study
(Pan et al. 2017)	· Influenza A H1N1 · Influenza A H3N2 · Influenza B Victoria · Respiratory Syncytial Virus-A · Adenovirus · Coronavirus 229E · Coronavirus NL63 · Human parainfluenza virus-2 · Human parainfluenza virus-3 · Human parainfluenza virus-4a · Influenza A · Influenza B · Coronavirus · Adenovirus	· 60	· 8	· 20	· ELISA · PCR	· Field sampling
(Nguyen et al. 2017)	· SARS-CoV-2 · Bovine Coronavirus (N/A)	· 60	· 8	· 15	· PCR	· Field sampling
(Kenarkoobi et al. 2020) (Hoff et al. 2022)	· SARS-CoV-2 · Bovine Coronavirus (N/A)	· 180 · 15	· 12 · 11.18	· 15 · 20	· PCR · TCID ₅₀ assay	· Field sampling · Inactivation study
This study	· MS2 (5.0×10^8 PFU/mL, 5.6×10^8 PFU/mL, 4.7×10^4 PFU/mL) · Influenza A H1N1 (4.6×10^6 gene copies/mL, 6.0×10^7 gene copies/mL)	· 10/60/360	· 4.0/8.0/10.0/ 12.5/13.3*	· 13 · 20	· Plaque assay · PCR	· Evaluation of the BioSampler

Conc.: Concentration. ELISA: Enzyme linked immunosorbent assay. PCR: Polymerase chain reaction. PFU: Plaque-forming units. SMPS: Scanning mobility particle sizer. TCID₅₀: 50% tissue culture infectious dose. *: These standard flow rates, measured at the inlet of the BioSampler, corresponded to 4.0/8.1/11.3/17.6/23.5 L/min at the outlet, respectively.

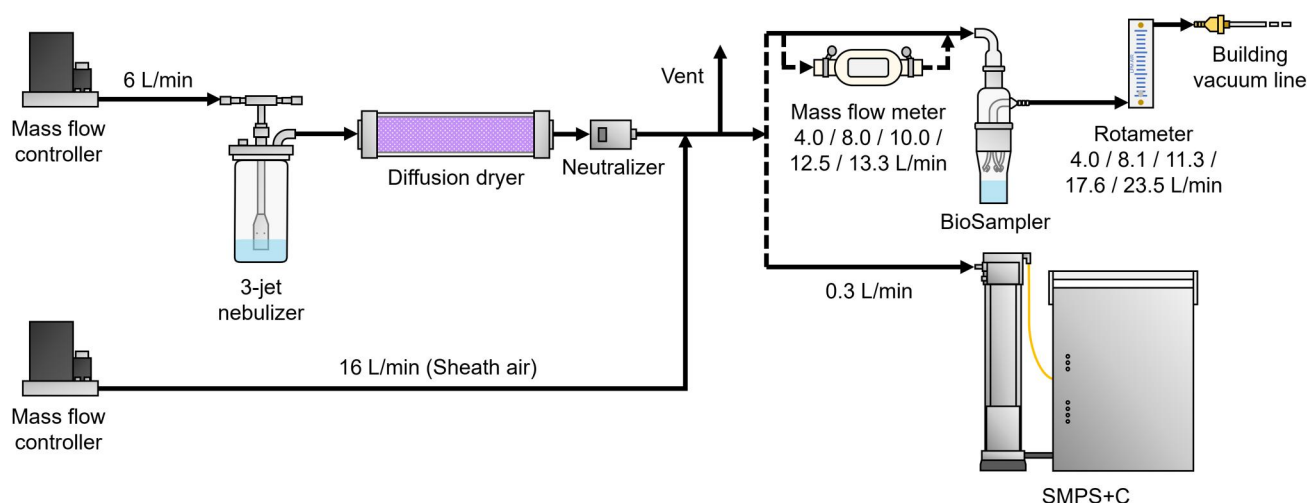


Figure 1. Schematic of the experimental setup for measuring the concentration of airborne viruses collected with the SKC BioSampler and the particle size distribution of airborne virus particles at the inlet of the BioSampler.

in laboratory-scale experiments (Verreault et al. 2008; Zuo et al. 2014). It has a diameter of 27 nm with an icosahedral structure. A suspension of MS2 virus, whose host is *Escherichia coli* C3000, was prepared for nebulization, as done in our previous studies (Bhardwaj et al. 2023; Jang et al. 2023; Lee et al. 2024). Briefly, the double-layer agar method was used to propagate MS2 bacteriophages (see the [online supplementary information \[SI\] Text S1](#)). After incubation for 8 h, the soft agar was scraped from the agar plate, mixed with deionized (DI) water in a 50-mL conical tube, and centrifuged at 1500 rpm for 25 min. Subsequently, the supernatant was extracted using a syringe and filtered with a 0.22- μm Millipore filter (4612, Pall Corporation, USA) to remove agar, bacteria, Luria-Bertani medium, and any debris. The virus suspensions were prepared at concentrations of $5.0 (\pm 1.9) \times 10^8$ PFU/mL (for the higher virus concentration in the nebulizer), $5.6 (\pm 2.3) \times 10^6$ PFU/mL (for the medium virus concentration), and $4.7 (\pm 2.6) \times 10^4$ PFU/mL (for the lower virus concentration) in 30 mL of DI water.

Influenza A virus H1N1 (KBPV-VR-76, South Korea) was purchased from the Korea Bank for Pathogenic Viruses (KBPV) and used in the present study. According to the KBPV, influenza A viruses were propagated in Madin-Darby canine kidney (MDCK) cells maintained in MEM supplemented with 2 $\mu\text{g}/\text{mL}$ of TPCK-trypsin. The cells were incubated at 35 °C with 5% CO₂, and cytopathic effect was monitored over a period of 2–4 days. For viral titration, MDCK cells were similarly cultured under identical conditions, and viral titers were determined after 4 days of incubation using plaque assay. The resulting virus stock showed 2.0×10^8 PFU/mL. Influenza A virus suspensions were diluted to $4.6 (\pm 1.6) \times 10^6$ gene copies/mL (for the higher virus concentration)

and $6.0 (\pm 2.3) \times 10^5$ gene copies/mL (for the lower virus concentration) in 30 mL of DI water.

2.2. Measurements of sampling flow rates

As the BioSampler operates under vacuum at high sampling flow rates, the flow rates at the inlet and outlet of the BioSampler were measured using a mass flow meter (4040, TSI Inc., MN, USA) and a rotameter (320-530, SKC Inc., PA, USA), respectively, before starting the experiments. Flow rates of 4.0, 8.0, 10.0, 12.5, and 13.3 Standard L/min (SLPM) corresponded to 4.0, 8.1, 11.3, 17.6, and 23.5 L/min at the outlet, respectively (Figure 1 and Figure S1). The relative difference in the volumetric flow rates between the standard condition and the inlet was 1.48%. The standard deviations of the measurements were ≤ 0.01 SLPM at all tested flow rates. At a flow rate of approximately 10.0 SLPM, the discrepancy in volumetric flow rate measurements between the inlet and outlet began to increase. The maximum achievable sampling flow rate in the BioSampler for this experimental setup (e.g., 20 or 13 mL of collection liquid and building vacuum line) was 13.3 SLPM where flow velocity through the nozzles approached the speed of sound (Fox et al. 2020), as observed in a previous study (Turgeon et al. 2014). The lowest pressures of the building vacuum line with and without the setup were 31.4 and 22.6 kPa, respectively.

2.3. Experimental procedures

Two types of experiments were conducted in the present study. In the first experiment, airborne MS2 viruses were collected using the BioSampler. The viable virus concentrations in the collected samples were measured using the plaque assay at various sampling

flow rates (4.0, 8.0, 10.0, 12.5, and 13.3 SLPM) and periods (10, 60, and 360 min) under different virus concentrations in the nebulizer (5.0×10^8 , 5.6×10^6 , and 4.7×10^4 PFU/mL) at 20-mL collection liquid. We selected a 20-mL sampling cup to ensure a sufficient amount of collection liquids for extended sampling periods, such as 360 min (Han and Mainelis 2012). Moreover, airborne influenza A viruses were collected at sampling flow rates of 10.0, 12.5, and 13.3 SLPM for 60 min under concentrations of 4.6×10^6 and 6.0×10^5 gene copies/mL at 20- and 13-mL collection liquids. In the second experiment, the virus concentrations at the inlet of the BioSampler were measured using gelatin filters or a water condensation-based sampler.

In the first experiment, a three-jet Collison nebulizer (CH Technologies, NJ, USA) containing a 30-mL virus suspension was supplied with clean air at 6 L/min and 20 psig to generate virus aerosol particles. After passing through a diffusion dryer (HCT, South Korea), the particles were neutralized using a neutralizer (5622, GRIMM, Germany). Sheath air at 16 L/min was added to achieve a total flow rate of 22 L/min. A built-in vacuum line of the laboratory building was utilized to vary the sampling flow rate in the BioSampler, and $1 \times$ phosphate-buffered saline (PBS) (pH 7.4, Gibco) was used as the collection medium. After sampling was completed, all samples in the BioSampler were swirled clockwise for three seconds (six turns) followed by counterclockwise swirling for three seconds (six turns), in order to minimize the particle losses on the inner surface of the sampler. The collected virus samples were transferred to 50-mL conical tubes or 1.5-mL microcentrifuge tubes, and stored at 4 °C for up to 8 h for the plaque assay or RT-qPCR assay (SI Text S2 and Figure S2). The viability of MS2 viruses did not reduce significantly during 10-h storage at 4 °C in a refrigerator (Figure S3). The temperature and relative humidity of the sampling flow during the experiments were 21.7 ± 1.1 °C and $32.9 \pm 1.6\%$, respectively. The size distributions of the generated virus aerosol particles were measured at the BioSampler inlet using SMPS+C (5416, GRIMM, Germany). During the 6-h sampling tests, the virus suspension in the nebulizer was replaced with a fresh one every hour. The BioSampler was also replenished with fresh PBS at the same time to maintain a 20-mL volume (Figure 1).

To find the virus concentrations at the inlet of the BioSampler, airborne MS2 viruses were collected at the inlet of the BioSampler in a similar manner as previously conducted (Lee et al. 2024) and their concentrations were measured using the plaque assay.

Briefly, the Button aerosol sampler (225-360, SKC, USA) equipped with a gelatin filter (25 mm, Sartorius, Germany) and a calibration adapter (225-361, SKC, USA) was used, where a flow rate of 6 L/min corresponding to a face velocity of 0.2 m/s was used since the manufacturer reported no significant differences in the recovery rates of T1 and T3 bacteriophages at inlet velocities of up to 0.4 m/s (Jaschhof 1992). The physical collection efficiency of the gelatin filter in the present study was measured to be 99.7% (data not shown), consistent with previous findings (Burton et al. 2007). After performing sampling for 1 min, the gelatin filters detached from the Button aerosol sampler were placed into 50-mL conical tubes with 1 mL of $1 \times$ PBS each, and shaken vigorously for 15 s. These suspensions were warmed immediately in a shaking incubator at 37 °C for 10 min to dissolve the gelatin filters completely. The virus concentrations at the inlet of the BioSampler were calculated using the equations provided in section 2.4.

The concentrations of airborne influenza A H1N1 viruses at the inlet of the BioSampler were also measured using the growth-based virus aerosol concentrator (GVC) (Jang et al. 2022) and RT-qPCR. Briefly, airborne influenza viruses were generated at 6 L/min, passed through a diffusion dryer and a neutralizer, diluted with 7 L/min of clean air, and then sampled at 6 L/min *via* impaction under the condition of 5 °C conditioner and 45 °C initiator. After sampling for 10 min, collected samples were eluted with 0.5-mL $1 \times$ PBS to conduct RT-qPCR assay.

2.4. Evaluation of airborne virus sampling

In the present study, relative infectious virus concentrations (RIVCs) and relative total virus concentrations (RTVCs) were measured for MS2 and influenza A viruses, respectively, as given by Hong et al. (2016)

$$RIVC = \frac{PFU_{sampler}}{PFU_{nebulizer}} \quad \text{and} \quad RTVC = \frac{qPCR_{sampler}}{qPCR_{nebulizer}} \quad (1)$$

where $PFU_{sampler}$ and $PFU_{nebulizer}$ indicate the concentrations of viable MS2 viruses (PFU/mL) in the collected samples and virus suspensions in the nebulizer, respectively. Moreover, $qPCR_{sampler}$ and $qPCR_{nebulizer}$ indicate the genomic copy number concentrations (gene copies/mL) in the collected samples and virus suspensions in the nebulizer, respectively. The virus concentrations in the nebulizer were measured at the beginning and end of the experiments, and their average values were used as the concentrations of virus suspensions. High RIVCs are favorable for rapid or

on-site virus measurement using immunoassay (Bhardwaj et al. 2020; Lee et al. 2022, 2023; Park et al. 2025) where further concentration techniques such as ultrafiltration and ultracentrifugation are usually unavailable, and intact virus antigens are used in the measurement. The ratio of RIVC to RTVC (or the PFU-to-gene copy ratio) shows a viable virus percentage through aerosol generation and sampling relative to that in the suspension (Jang et al. 2022).

The intrinsic collection efficiency (η_i) was also measured and shows how many of incoming viruses can be captured in the collection medium of the BioSampler, which can be computed by

$$\eta_i = \frac{N_{collected}}{N_{inlet}} \quad (2)$$

where $N_{collected}$ and N_{inlet} refer to the numbers of viruses (PFU or gene copies) that remain in the collection liquid of the BioSampler after sampling and that enter the BioSampler during sampling, respectively.

The concentration of airborne viruses at the BioSampler inlet (C_{air} ; PFU/L or gene copies/L) was computed by

$$C_{air} = \frac{N_{collected}}{Q \times \eta \times t} \times \frac{6 \text{ or } 13}{22} \quad (3)$$

where $N_{collected}$, Q , η , t , 6, 13, and 22 indicate the number of viruses collected (PFU or gene copies) in a gelatin filter or the GVC during a sampling period, flow rate (L/min), collection efficiency (%), sampling period (min) of a gelatin filter or the GVC, flow rates for the gelatin filter and GVC experiments, and flow rate at the inlet of the BioSampler, respectively.

The plaque count in the present study was denoted as “not detected (N.D.)” if the number of PFUs was less than 10 for more than half of the samples measured in each case because in general, plaques can be counted reliably when their numbers are in the range of 10–100 (Cormier and Janes 2014) or 30–300 (Vass et al. 2024).

2.5. Statistical analysis

The normality of the dataset was confirmed using the Shapiro-Wilk test. Student’s t -test or analysis of variance followed by Tukey’s multiple comparison test using OriginPro 2020 was used to analyze the data statistically. The differences were considered significant if the p -value was <0.05 (95% confidence interval). If not, they were considered n.s. (not significant).

3. Results and discussion

3.1. Collection of MS2 viruses at various sampling flow rates for 10-min sampling and 20-mL collection liquid

Figure 2a shows RIVCs of MS2 viruses collected in the BioSampler at various sampling flow rates for the higher, medium, and lower virus concentrations in the nebulizer during 10-min sampling. RIVCs increased with an increase in virus concentrations in the nebulizer. This may be attributed to the fact that more virus particles with larger particle diameters were generated from the nebulizer as the virus concentration in the nebulizer increased. As the virus concentration in the nebulizer increased, the peak diameter of the particle size distribution at the inlet of the BioSampler and the number concentrations of most particle sizes increased; the peak diameter of the relative particle size distribution for the medium and lower concentrations was approximately 40 nm and that for the higher and medium concentrations was approximately 240 nm (Figure S4). This may lead to increased collection of virus particles with increased virus concentrations in the nebulizer, according to the collection efficiencies reported in a previous study (Li et al. 2018), where the collection efficiency of the BioSampler increased as the particle diameter increased beyond 40 nm.

The size distribution of test aerosol particles is critical to the characterization of an air sampler. In most previous studies on airborne virus experiments, the mass median diameters (MMDs) ranged from tens of nanometers to around $10 \mu\text{m}$, and the wide range may be due to differences in their experimental conditions, such as nebulizer type and flow rate, nebulizing medium and its composition, and the use of aerosol chambers or sheath flow. In this study, the MMD for MS2 virus aerosol particles generated was 99 nm (Figure 2b). In fact, viruses are enriched in small aerosols ($<5 \mu\text{m}$), and a large number fraction is submicrometer-sized in most respiratory activities (Wang et al. 2021). Moreover, the SKC BioSampler shows low collection efficiencies for submicrometer-sized airborne virus particles, which are important for characterizing the BioSampler for detection of airborne respiratory viruses.

At the higher and medium virus concentrations in the nebulizer, RIVCs increased as the flow rate increased from 4.0 SLPM and 8.0 SLPM, respectively, to 13.3 SLPM (Figure 2a). At the higher virus concentration in the nebulizer, viruses were detected in the samples at all tested sampling flow rates, with the RIVC increasing from 1.32×10^{-5} at 4.0 SLPM to

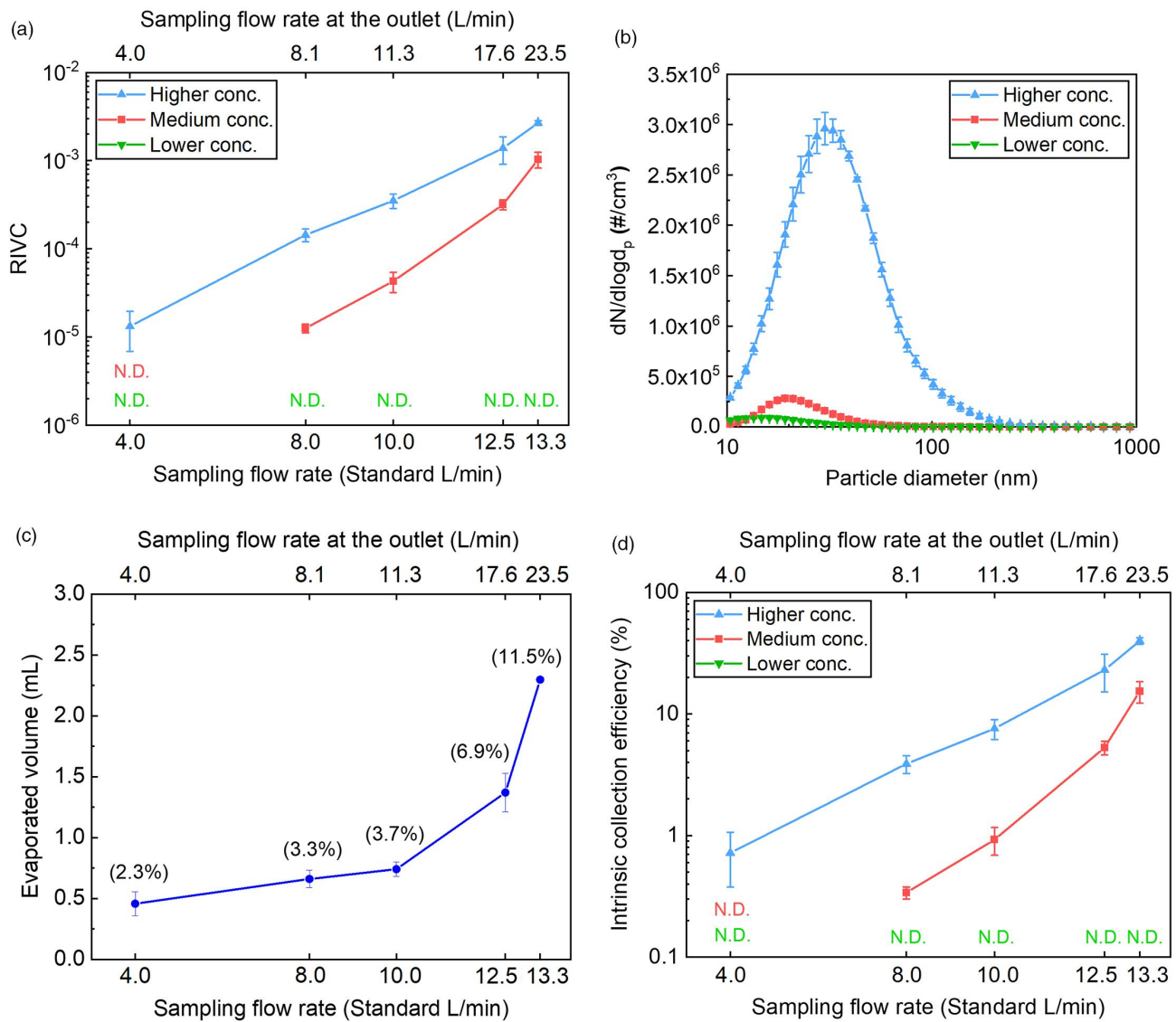


Figure 2. (a) RIVC of MS2 viruses, (b) particle size distribution of generated aerosol particles for each MS2 virus concentration in the nebulizer, (c) evaporated volume of the collection medium (PBS), and (d) intrinsic collection efficiency of viable MS2 viruses with the sampling flow rate (4.0–13.3 SLPM) at various virus concentrations in the nebulizer for 10-min sampling. The data points represent the average values of three measurements with their standard deviations. Higher concentration in the nebulizer: $5.0 (\pm 1.9) \times 10^8$ PFU/mL. Medium concentration in the nebulizer: $5.6 (\pm 2.3) \times 10^6$ PFU/mL. Lower concentration in the nebulizer: $4.7 (\pm 2.6) \times 10^4$ PFU/mL. Conc.: Concentration. Plaque measurements at all the tested flow rates for the lower concentration and 4.0 SLPM for the medium concentration were indicated as N.D.

2.68×10^{-3} at 13.3 SLPM. Notably, the RIVC was higher at 13.3 SLPM than at 12.5 SLPM ($p < 0.001$), where the PFU concentration of the collected samples increased by 2.86 times despite a small increase (6.4%) in the flow rate. This finding is particularly interesting considering that the manufacturer recommends 12.5 SLPM as the flow rate for the BioSampler. At the medium virus concentration in the nebulizer, the same trend was observed; however, the RIVC was lower. The RIVC increased from 1.26×10^{-5} at 8.0 SLPM to 1.03×10^{-3} at 13.3 SLPM, and the plaque

count at 4.0 SLPM was N.D. Moreover, the RIVC at 13.3 SLPM was higher than that at 12.5 SLPM ($p < 0.0001$), where the PFU concentration of collected samples was 3.89 times higher at 13.3 SLPM. This suggests that the BioSampler can capture more viable viruses at flow rates higher than 12.5 SLPM.

A possible explanation for this observation may be that more airborne virus particles can enter the BioSampler at a higher flow rate. Thus, the RIVC was normalized with the flow rate to exclude such an effect (Figure S5). The RIVC/SLPM values at 13.3

SLPM were also higher than those at 12.5 SLPM at the higher and medium virus concentrations in the nebulizer ($p = 0.001$ and $p < 0.001$, respectively).

Another possible reason why the RIVC at 13.3 SLPM was higher than that at 12.5 SLPM may be the increased evaporative losses in the collection medium at a higher sampling flow rate. The evaporative losses were measured at varying flow rates during 10-min sampling, and they were found to increase with the flow rate (Figure 2c). The evaporative loss in the collection medium at 13.3 SLPM was 0.93 mL more than that at 12.5 SLPM, corresponding to a 5.25% increase in the concentration, whereas RIVCs at 13.3 SLPM were 93% and 225% higher than those at 12.5 SLPM for the higher and medium virus concentrations in the nebulizer, respectively. Thus, the evaporative loss may not contribute much to the higher RIVC at 13.3 SLPM.

Unlike the aforementioned results, MS2 viruses were N.D. in the BioSampler at the lower virus concentration in the nebulizer during 10-min sampling at any sampling flow rate tested in the present study. This may be because the number of virus particles generated in the nebulizer, including viable viruses, was significantly lower than in the other two cases (Figure S4) and/or the sampling time was not sufficiently long. We measured the concentrations of airborne viable MS2 viruses at the inlet of the BioSampler using gelatin filters at the higher, medium, and lower virus concentrations in the nebulizer, which corresponded to 4.4×10^8 , 5.0×10^6 , and 4.2×10^4 PFU/m³ of air, respectively. In the lowest concentration case, the virus concentration was within the concentrations of respiratory viruses measured in the field. In particular, the airborne viable SARS-CoV-2 concentrations in a residential setting were measured to be 3.85×10^3 to 2.92×10^5 PFU/m³ (Vass et al. 2022; 2023). These airborne virus concentrations at the inlet were used to compute the intrinsic collection efficiencies.

The same trends as RIVCs were observed for the intrinsic collection efficiency (Figure 2d). The intrinsic collection efficiency increased as the sampling flow rate and virus concentration in the nebulizer increased. The intrinsic collection efficiency ranged up to 39.8% and 15.3% at 13.3 SLPM for the higher and medium virus concentrations in the nebulizer during 10-min sampling, respectively. The intrinsic collection efficiencies at 12.5 SLPM for the higher and medium virus concentrations in the nebulizer were 23.1% and 5.3%, respectively. The intrinsic collection efficiencies at 13.3 SLPM were higher than those at 12.5 SLPM at the

higher and medium virus concentrations in the nebulizer ($p = 0.002$ and $p < 0.001$, respectively). The sensitivity of the collection efficiency with respect to flow rate also increased with the flow rate. At higher flow rates (e.g., 12.5–13.3 SLPM), a small increase in the sampling flow rate caused a large increase in the collection efficiency for the investigated particle sizes, contrasting with less steep increases in the collection efficiencies at smaller flow rates.

In general, the collection efficiency of particles in impingers depends crucially on the flow rate. Numerous studies have revealed that the collection efficiencies of various impingers, including the BioSampler, AGI-4, and AGI-30, do not necessarily increase with the sampling flow rate (Grinshpun et al. 1997; Hogan et al. 2005; Dart and Thornburg 2008; Wei et al. 2010; Yu et al. 2016; Zheng and Yao 2017). However, in the present study, the intrinsic collection efficiency of the BioSampler increased with the sampling flow rate; these values were significantly higher at 13.3 SLPM than at 12.5 SLPM for 10-min sampling periods in 20 mL of collection liquid.

This discrepancy may be attributed to the following reasons. Firstly, different types of impingers were used in the studies. Dart and Thornburg (2008) employed the G-S impinger, Grinshpun et al. (1997) used AGI-4 and AGI-30, Wei et al. (2010) used the midjet impinger, and Yu et al. (2016) utilized AGI-30. In these impingers, airborne particles are collected *via* inertial impaction using vertical nozzles, which is different from swirling-based collection using tangential nozzles in the BioSampler, where particle bounce and reaerosolization are significantly reduced (Willeke et al. 1998). Secondly, different-sized particles or different types of particles were used in the BioSamplers, which might have contributed to differences in the results. For example, Hogan et al. (2005) found that for 25 nm diameter particles, collection efficiency did not increase with sampling flow rate due to a transition from Brownian motion to turbulent diffusion during collection. However, for 300 nm diameter particles, collection efficiency increased with flow rate. Considering that the collection efficiency of the BioSampler increased as the particle diameter increased beyond 40 nm (Li et al. 2018), the data for 300 nm particles might have played a more dominant influence on airborne virus sampling in the present study. Zheng and Yao (2017) investigated collection of indoor bioaerosol particles rather than airborne viruses only. Moreover, the method used in this study to calculate the intrinsic collection efficiency was based on measuring the PFU or gene copies of

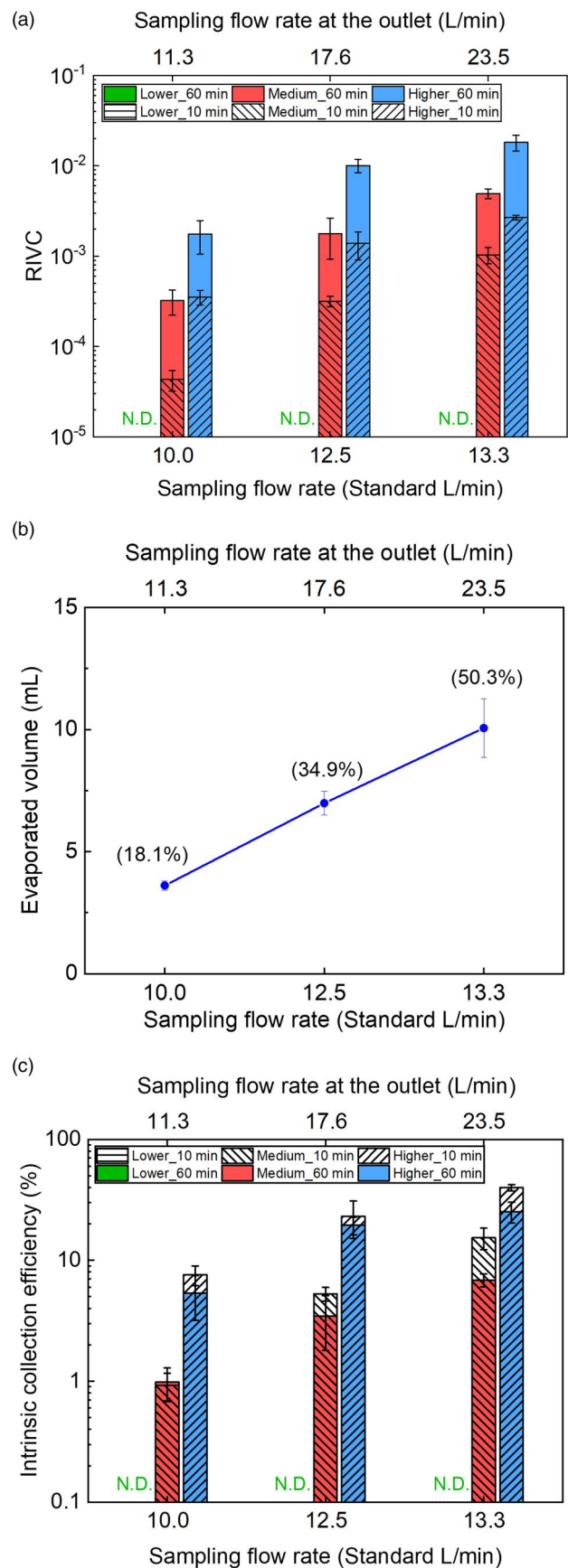
airborne viruses, rather than counting aerosol particles *via* DMA and CPC (Hogan et al. 2005) or UV-APS (Zheng and Yao 2017).

3.2. Collection of MS2 viruses at various sampling periods for 20-mL collection liquid

Figure 3a and S6 show the RIVCs and RIVC/SLPM at 10.0, 12.5, and 13.3 SLPM during 60-min sampling for the higher, medium, and lower virus concentrations in the nebulizer, respectively. As the virus concentration in the nebulizer and the sampling flow rate increased, the RIVC during 60-min sampling also increased. For the higher and medium concentrations in the nebulizer, the RIVC ($p=0.012$ and 0.002 , respectively) was higher at 13.3 SLPM than at 12.5 SLPM, where the PFU concentrations in the collected samples were 2.12 and 3.85 times higher at 13.3 SLPM for the higher and medium concentrations in the nebulizer, respectively. These results are in line with those obtained during 10-min sampling and can be attributed to the greater number of particles generated at higher concentrations in the nebulizer and enhanced inertial forces at increased flow rates. The BioSampler was not effective in collecting detectable airborne virus particles at the lower virus concentration in the nebulizer or 4.2×10^4 PFU/m³ of air.

Moreover, the average RIVCs of 10.0, 12.5, and 13.3 SLPM during 60-min sampling were 6.79 and 5.06 times higher than those during 10-min sampling for the higher and medium concentrations in the nebulizer, respectively. These sixfold increases appear to be consistent with the sixfold longer sampling period. However, considering the significant evaporation of the collection medium (Figure 3b), the RIVCs during 60-min sampling were lower than the expected values. That is, the RIVC will be 7.32 to 12.08 times higher during 60-min sampling as the flow rate increases from 10.0 to 13.3 SLPM if only the sampling period and evaporated volume are considered.

A possible reason for the differences is that collection efficiency in the BioSampler for infectious MS2 viruses decreased as the surface level of the collection medium dropped or sampling time increased from 10 min to 60 min (Figure 3c). In fact, the ratio of the RIVC to the intrinsic collection efficiency is inversely proportional to the volume of the collection medium after sampling. In the case of 10-min sampling, the evaporated volume in the collection medium did not contribute greatly to increases in the concentrations of



samples with the flow rate. The increases in concentration owing to evaporation only were 13% at 13.3 SLPM and 3.8% at 10 SLPM. However, in the case of 60-min sampling, the volumes evaporated were much larger. The increases in concentration owing to evaporation only compared to 20-mL collection liquids were 101.3% at 13.3 SLPM and 22.1% at 10 SLPM. The intrinsic collection efficiencies at 12.5 SLPM for the higher and medium virus concentrations in the nebulizer after 60-min samplings dropped to 19.5% and 3.5%, respectively. The intrinsic collection efficiencies at 13.3 SLPM for the higher and medium virus concentrations in the nebulizer after 60-min samplings also decreased to 25.3% and 6.9%, respectively. The differences in the intrinsic collection efficiency between 10 and 60 min were significant at 13.3 SLPM ($p=0.01$) but not at 12.5 SLPM ($p>0.15$). Thus, the number of infectious MS2 viruses collected may not increase linearly with the sampling time.

One of the reasons for the reduced collection of infectious MS2 viruses at 60-min sampling may be that the mechanical impact induced by high nozzle velocity (as high as the speed of sound) in the BioSampler can lead to a loss of viability of air-sampled viruses. To investigate this possibility, the PFU-to-gene copy ratios during aerosol generation and air sampling were measured for 10- and 60-min samplings at 13.3 SLPM and the medium concentration in the nebulizer. The measurements demonstrated that the PFU-to-gene-copy ratio decreased from 0.54 ± 0.05 after 10-min sampling to 0.38 ± 0.09 after 60-min samplings, indicating that the viable virus percentage of sampled viruses decreased with sampling period, although MS2 viruses are recognized as one of the most resistant viruses during sampling (Turgeon et al. 2014).

The collected virus particles may also escape *via* reaerosolization. Presently, no works on the reaerosolization of viruses in the BioSampler are available. Measurements using an AGI-30 impinger revealed that the reaerosolization of MS2 viruses was significant in a range of 10^2 to

10^6 PFU/mL and increased with the flow rate; however, the reaerosolization of polystyrene latex (PSL) particles was significantly lower in the BioSampler than in AGI-30 impinger (Willeke et al. 1998; Riemenschneider et al. 2010). The reaerosolization of $0.9 \mu\text{m}$ PSL particles in the BioSampler were less than 1% of the particle concentration in the collection liquid (Han and Mainelis 2012). Moreover, the particles attached to the inner surface of the sampler may not be recovered for measurement (internal losses) (Han and Mainelis 2012), which were not evaluated in this study.

In addition, 360-min sampling experiments were conducted for application to field measurements (Figure 4), where airborne virus sampling is usually performed over several hours (Memish et al. 2014; Kenarkoohi et al. 2020; Sousan et al. 2022) and the virus concentration in the air is usually low. The virus concentration in the nebulizer was 4.7×10^4 PFU/mL, corresponding to 4.2×10^4 PFU/ m^3 of air. The sampling flow rates were 10.0, 12.5, and 13.3 SLPM. During 360-min sampling, detectable MS2 virus concentrations were noted at these three flow rates, with the RIVC increasing from 5.44×10^{-4} to 2.65×10^{-3} , and the RIVC was higher at 13.3 SLPM than at 12.5 SLPM ($p < 0.001$). However, the intrinsic collection efficiencies for infectious MS2 viruses over 360-min sampling at these flow rates were very low (0.3% – 1.0%) (Figure 4b).

Unlike a previous finding that 6 and 9 L/min were more efficient than 12.5 L/min for airborne MS2 virus sampling using the BioSampler (Anwar et al. 2010), we found that 13.3 SLPM was the most efficient flow rate during 10-, 60-, and 360-min sampling periods. This discrepancy may arise from the different experimental setups in these two studies. Anwar et al. (2010) used a fixed virus-laden flow of 5 L/min and a varying dilution air flow rate of 1 to 20 L/min for a sampling flow rate of 3 to 12.5 L/min to compare AGI-30 with the BioSampler. Consequently, the airborne virus concentration at the inlet might have been higher at a lower sampling flow rate. In the present study, both nebulization and dilution air flow rates were fixed. Hence, the airborne virus concentrations at the inlet of the BioSampler were constant regardless of its sampling flow rate.

3.3. Collection of influenza viruses during 60-min sampling for 20-mL collection liquid

Airborne influenza A viruses were also collected for 60 min and quantified using RT-qPCR (Figure 5a and Figure S7); the limit of detection was approximately 200 copies/mL and the MMD for the influenza virus

Figure 3. (a) RIVC of MS2 viruses, (b) evaporated volume of collection medium (PBS), and (c) intrinsic collection efficiencies of viable MS2 viruses for 60-min sampling at various virus concentrations in the nebulizer. RIVCs for 10-min sampling were also displayed for comparison. The data points represent the average values of three measurements with their standard deviations. Higher concentration in the nebulizer: $5.0 (\pm 1.9) \times 10^8$ PFU/mL. Medium concentration in the nebulizer: $5.6 (\pm 2.3) \times 10^6$ PFU/mL. Lower concentration in the nebulizer: $4.7 (\pm 2.6) \times 10^4$ PFU/mL. Plaque measurements at 10.0, 12.5, and 13.3 SLPM during 10- and 60-min samplings for the lower concentration in the nebulizer were indicated as N.D.

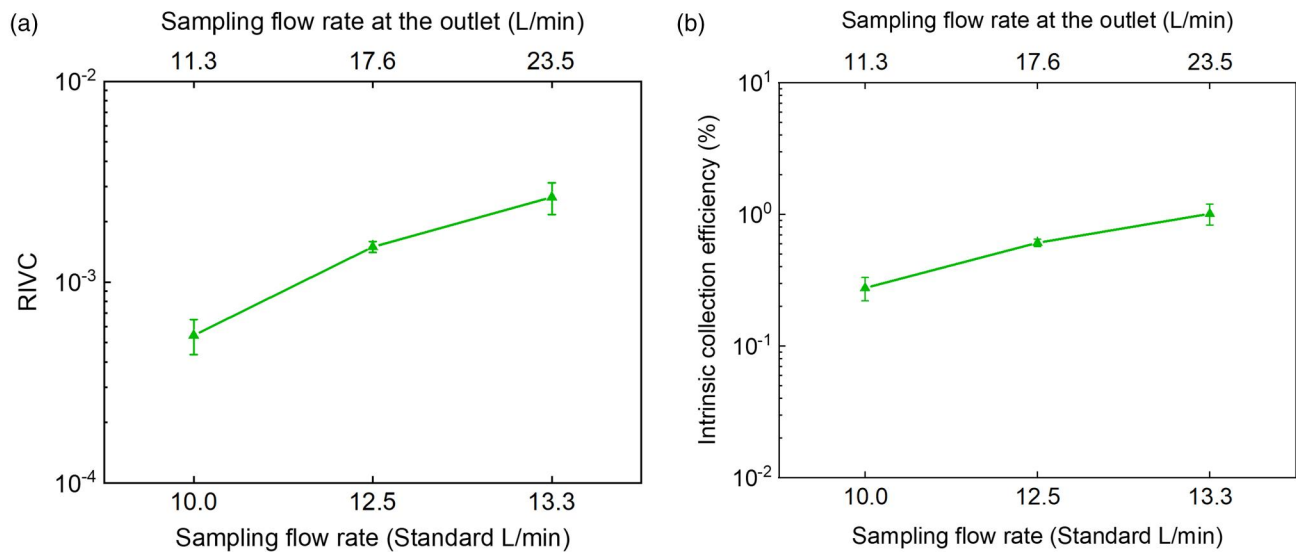


Figure 4. (a) RIVC and (b) intrinsic collection efficiencies of viable MS2 viruses for 360-min sampling at 10.0, 12.5 and 13.3 SLPM. The concentration in the nebulizer was $4.7 (\pm 2.6) \times 10^4$ PFU/mL corresponding to $4.2 (\pm 2.3) \times 10^4$ PFU/m³ of air. The data points represent the average values of three measurements with their standard deviations.

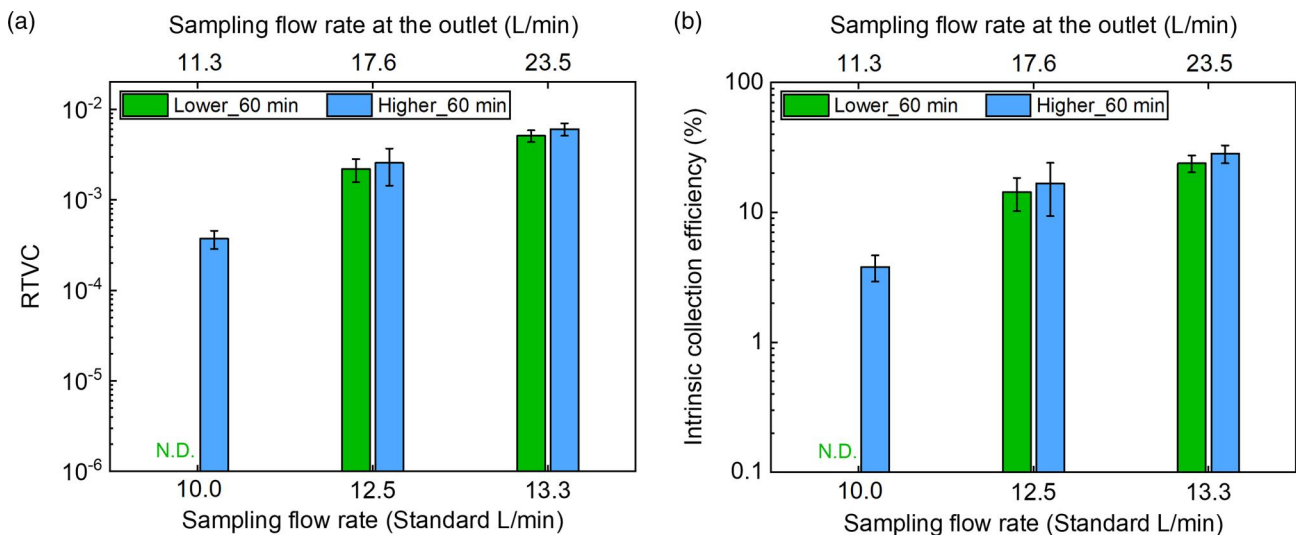


Figure 5. (a) RTVC and (b) intrinsic collection efficiencies of influenza A virus H1N1 for 60-min sampling at various virus concentrations in the nebulizer. The data points represent the average values of three measurements with their standard deviations. Higher concentration in the nebulizer: $4.6 (\pm 1.6) \times 10^6$ gene copies/mL corresponding to $1.2 (\pm 0.4) \times 10^6$ gene copies/m³ of air. Lower concentration in the nebulizer: $6.0 (\pm 0.2) \times 10^5$ gene copies/mL corresponding to $1.6 (\pm 0.6) \times 10^5$ gene copies/m³ of air. PCR assay results at 10 SLPM for the lower concentration in the nebulizer were indicated as N.D.

aerosol particles generated was 45 nm (Figure S8). Two airborne virus concentrations were selected based on previous studies: 1.2×10^6 gene copies/m³ (higher concentration) and 1.6×10^5 gene copies/m³ (lower concentration) (Shiu et al. 2020; Chamseddine et al. 2021; Dubuis et al. 2021; Park et al. 2025). For the higher and lower virus concentrations in the nebulizer, the RTVCs ($p=0.006$ and 0.007 , respectively) were significantly higher at 13.3 SLPM than at 12.5 SLPM. This result may be attributed to the greater number of particles entering the sampler at a higher

flow rate and enhanced particle inertia at higher flow rates, consistent with the observations for MS2 viruses.

The intrinsic collection efficiencies were higher at higher flow rate, albeit not significantly different ($p=0.065$) between 12.5 SLPM and 13.3 SLPM at the higher concentration case, and p -values were 0.038 at the lower concentration case (Figure 5b). The intrinsic collection efficiencies at a concentration of 1.6×10^5 gene copies/m³ of air were 14.3% and 23.8% at 12.5 SLPM and 13.3 SLPM, respectively. Collection

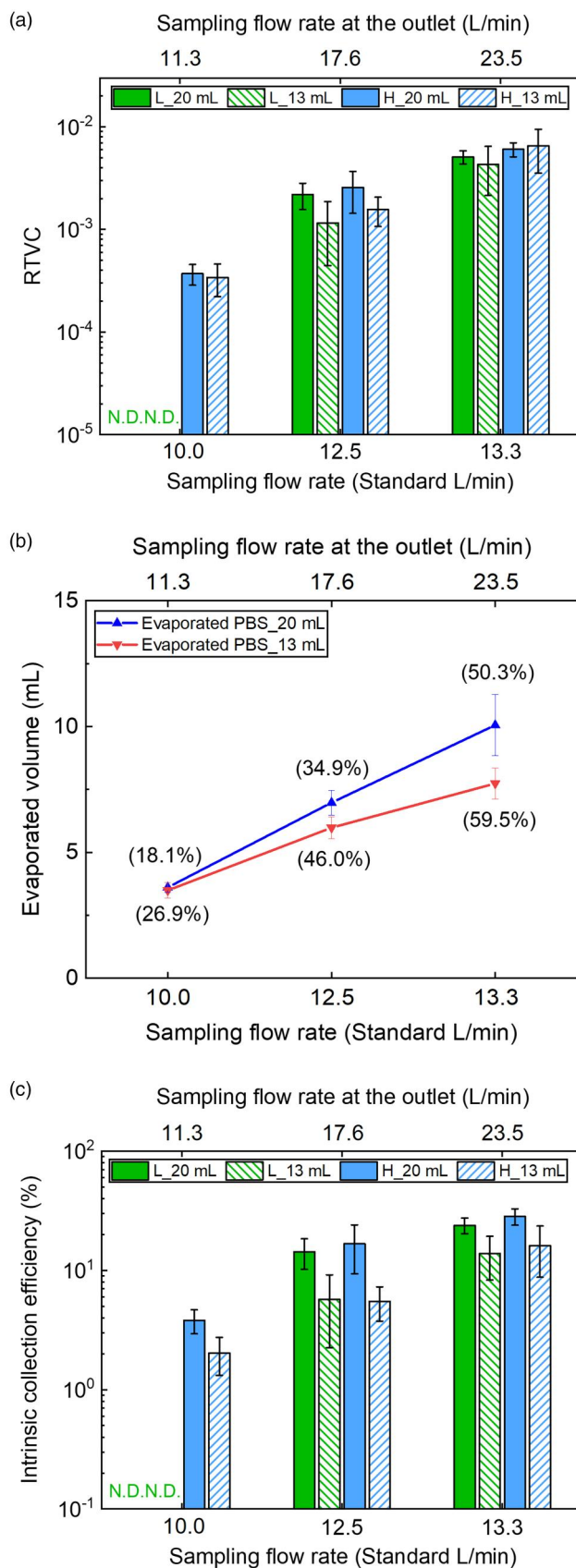


Figure 6. (a) RTVC of influenza A virus H1N1 for 60-min sampling at two virus concentrations in the nebulizer at the collection liquid volumes of 20 and 13 mL, (b) evaporated volume of

efficiencies of influenza viruses for the BioSampler were presented in only a few studies although the BioSampler has been extensively used. Unlike the data presented using RT-qPCR in the current study, Li et al. (2018) reported collection efficiencies of 0.5–5% for infectious influenza viruses at 12.5 L/min and a 5-mL sampling cup. Lednicky et al. (2016) also presented collection efficiencies of less than 8.6% for infectious influenza viruses at 6.86 L/min. These two collection efficiencies were based on the infectious virus concentrations in the suspensions, without a diffusion dryer. The enhanced efficiencies at 13.3 SLPM suggest that higher sampling flow rates can improve virus detection even at a field-level virus concentration in the air.

3.4. Collection of influenza viruses during 60-min sampling at a reduced collection volume

Airborne influenza A H1N1 viruses were also measured using 13 mL of collection liquid in order to evaluate the performance of the BioSampler during a 120-min sampling period (Figure 6a). The 13-mL volume was chosen to account for the 7.0-mL liquid evaporation out of 20-mL initial volume during 60-min sampling at 12.5 SLPM (Figure 6b). Consistent with previous experiments, two concentrations in the air (higher: 1.2×10^6 gene copies/m³ and lower: 1.6×10^5 gene copies/m³) were tested. Higher RTVCs were consistently observed at 13.3 SLPM compared to 12.5 SLPM at 13-mL collection liquid, with *p*-values being 0.031 and 0.075 for the higher and lower airborne virus concentrations, respectively. RTVCs and RTVC/SLPM (Figure S9) showed no significant differences (*p* > 0.13) between 13 mL and 20 mL at the two airborne virus concentrations and sampling flow rates (10.0, 12.5, and 13.3 SLPM).

The intrinsic collection efficiencies were also measured for 13 mL of collection liquid (Figure 6c). The intrinsic collection efficiencies of influenza viruses

PBS for the collection liquid volumes of 20 and 13 mL, and (c) intrinsic collection efficiencies of influenza A virus H1N1 for 60-min sampling at two virus concentrations in the nebulizer at the collection liquid volumes of 20 and 13 mL. The data points represent the average values of three measurements with their standard deviations. Hs in the legends denote higher concentration in the nebulizer: $4.6 (\pm 1.6) \times 10^6$ gene copies/mL corresponding to $1.2 (\pm 0.4) \times 10^6$ gene copies/m³ of air. Ls in the legends denote lower concentration in the nebulizer: $6.0 (\pm 0.2) \times 10^5$ gene copies/mL corresponding to $1.6 (\pm 0.6) \times 10^5$ gene copies/m³ of air. PCR assay results at 10 SLPM for the lower concentration in the nebulizer were indicated as N.D.

were lower at 13-mL compared to 20-mL case, although differences were not significant, and *p*-values were in the range of 0.05–0.07. This may be consistent with the findings of Zheng and Yao (2017). They measured collection efficiencies using UV-APS for indoor bioaerosols, and they observed increased collection efficiencies with increasing volume. However, for particles less than 0.5 μm , there were no significant differences in collection efficiencies ($p = 0.089$) between different collection volumes of 5, 10, and 20 mL at a sampling flow rate of 12.5 L/min, while significant differences were observed at the other sizes (0.5–10 μm) ($p < 0.01$).

4. Conclusions

In this study, we investigated the collection of airborne MS2 viruses using the BioSampler and plaque assay under varying virus concentrations in the nebulizer, sampling flow rates, and sampling periods. At higher and medium virus concentrations in the nebulizer, the RIVC and intrinsic collection efficiency for viable viruses increased with an increase in the flow rate during 10- and 60-min sampling. Interestingly, the RIVC and intrinsic collection efficiency at 13.3 SLPM were higher than those at the manufacturer-recommended sampling flow rate of 12.5 SLPM, albeit not significantly different at the following condition: higher virus concentrations in the nebulizer and 60-min sampling for the intrinsic collection efficiency. For the higher virus concentration in the nebulizer, MS2 viruses were detected across all tested flow rates during 10-min sampling; however, they were N.D. at 4.0 SLPM for the medium virus concentration in the nebulizer and at any tested flow rates for the lower virus concentration in the nebulizer, which corresponded to 4.2×10^4 PFU/ m^3 of air and was close to the field-level concentration of SARS-CoV-2 viruses. Based on these findings, 360-min sampling was also performed at the lower virus concentration in the nebulizer, and viable MS2 viruses were detected at flow rates of 10.0, 12.5, and 13.3 SLPM. Airborne influenza A viruses were also collected for 60 min at 20- and 13-mL collection volumes, and analyzed using RT-qPCR. The measured RTVCs of influenza A viruses increased with increasing flow rates and were higher at 13.3 SLPM than at 12.5 SLPM. The intrinsic collection efficiencies of influenza viruses were reduced at 13 mL compared to 20 mL, albeit not significantly different. The characterization of the BioSampler across various sampling flow rates, virus concentrations in the air, and sampling periods for

both MS2 and influenza viruses is expected to be valuable for future research on airborne virus sampling.

Author contribution

Chaewoon Jung: Methodology, Formal analysis, Investigation, Writing – Original Draft, Writing – Review & Editing. **Wonyoung Jeon:** Investigation. **Vidhurathan Soundararajan:** Methodology. **Jaesung Jang:** Formal analysis, Writing – Original Draft, Writing – Review & Editing, Supervision.

Disclosure statement

The authors declare that they have no known competing financial interests or personal relationships that could have influenced the work reported in this paper.

Funding

This work was supported by the National Research Foundation of Korea (NRF) grants (RS-2024-00341961) and by the Basic Science Research Program through the NRF funded by the Ministry of Education (RS-2020-NR049578).

Data availability

Data will be available from the corresponding author upon reasonable request.

References

- Anwar D, Oh S, Wu C. 2010. Virus collection efficiency of biosampler versus impinger with variable time and flow rate. University of Florida.
- Bhardwaj J et al. 2021. Recent advancements in the measurement of pathogenic airborne viruses. *J Hazard Mater.* 420:126574. <https://doi.org/10.1016/j.jhazmat.2021.126574>
- Bhardwaj J, Kim M-W, Jang J. 2020. Rapid airborne influenza virus quantification using an antibody-based electrochemical paper sensor and electrostatic particle concentrator. *Environ Sci Technol.* 54(17):10700–10712. <https://doi.org/10.1021/acs.est.0c00441>
- Bhardwaj J, Ngo ND, Lee J, Jang J. 2023. High enrichment and near real-time quantification of airborne viruses using a wet-paper-based electrochemical immunosensor under an electrostatic field. *J Hazard Mater.* 442:130006. <https://doi.org/10.1016/j.jhazmat.2022.130006>
- Burton NC, Grinshpun SA, Reponen T. 2007. Physical collection efficiency of filter materials for bacteria and viruses. *Ann Occup Hyg.* 51(2):143–151. <https://doi.org/10.1093/annhyg/mel073>
- Chamseddine A et al. 2021. Detection of influenza virus in air samples of patient rooms. *J Hosp Infect.* 108:33–42. <https://doi.org/10.1016/j.jhin.2020.10.020>
- Cormier J, Janes M. 2014. A double layer plaque assay using spread plate technique for enumeration of bacteriophage ms2. *J Virol Methods.* 196:86–92. <https://doi.org/10.1016/j.jviromet.2013.10.034>

- Dart A, Thornburg J. 2008. Collection efficiencies of bioaerosol impingers for virus-containing aerosols. *Atmos Environ.* 42(4):828–832. <https://doi.org/10.1016/j.atmosenv.2007.11.003>
- Doel C, Gloster J, Valarcher J. 2009. Airborne transmission of foot-and-mouth disease in pigs: Evaluation and optimisation of instrumentation and techniques. *Vet J.* 179: 219–224. <https://doi.org/10.1016/j.tvjl.2007.09.010>
- Dubuis M-E et al. 2021. High and low flowrate sampling of airborne influenza in hospital rooms during three outbreaks. *J Aerosol Sci.* 158:105824. <https://doi.org/10.1016/j.jaerosci.2021.105824>
- Fabian P, McDevitt J, Houseman E, Milton D. 2009. Airborne influenza virus detection with four aerosol samplers using molecular and infectivity assays: considerations for a new infectious virus aerosol sampler. *Indoor Air.* 19(5):433–441. <https://doi.org/10.1111/j.1600-0668.2009.00609.x>
- Fox RW, McDonald AT, Mitchell JW. 2020. Fox and McDonald's introduction to fluid mechanics 10th ed. John Wiley & Sons, Inc.
- Grinshpun SA et al. 1997. Effect of impaction, bounce and reaerosolization on the collection efficiency of impingers. *Aerosol Sci Technol.* 26(4):326–342. <https://doi.org/10.1080/02786829708965434>
- Han T, Mainelis G. 2012. Investigation of inherent and latent internal losses in liquid-based bioaerosol samplers. *J Aerosol Sci.* 45:58–68. <https://doi.org/10.1016/j.jaerosci.2011.11.001>
- Hoff B et al. 2022. Observed reductions in the infectivity of bioaerosols containing bovine coronavirus under repetitively pulsed RF exposure. *IEEE Trans Biomed Eng.* 70(2):640–649. <https://doi.org/10.1109/TBME.2022.3199333>
- Hogan C et al. 2005. Sampling methodologies and dosage assessment techniques for submicrometre and ultrafine virus aerosol particles. *J Appl Microbiol.* 99(6):1422–1434. <https://doi.org/10.1111/j.1365-2672.2005.02720.x>
- Hong S, Bhardwaj J, Han C-H, Jang J. 2016. Gentle sampling of submicrometer airborne virus particles using a personal electrostatic particle concentrator. *Environ Sci Technol.* 50(22):12365–12372. <https://doi.org/10.1021/acs.est.6b03464>
- Jang J, Bhardwaj J, Jang J. 2022. Efficient measurement of airborne viable viruses using the growth-based virus aerosol concentrator with high flow velocities. *J Hazard Mater.* 434:128873. <https://doi.org/10.1016/j.jhazmat.2022.128873>
- Jang J, Jeon W, Jang J. 2023. Effects of the nozzle-to-nozzle distance on the performance of the water condensation growth-based virus aerosol concentrator. *J Aerosol Sci.* 174:106247. <https://doi.org/10.1016/j.jaerosci.2023.106247>
- Jaschhof H. 1992. Sampling virus aerosols using the gelatin membrane filter. *Bio Tech.* 6:1–6.
- Jiang X et al. 2016. Use of RNA amplification and electrophoresis for studying virus aerosol collection efficiency and their comparison with plaque assays. *Electrophoresis.* 37(19):2574–2580. <https://doi.org/10.1002/elps.201600141>
- Kenarkoohi A et al. 2020. Hospital indoor air quality monitoring for the detection of SARS-COV-2 (Covid-19) virus. *Sci Total Environ.* 748:141324. <https://doi.org/10.1016/j.scitotenv.2020.141324>
- Kim HR, An S, Hwang J. 2021. High air flow-rate electrostatic sampler for the rapid monitoring of airborne coronavirus and influenza viruses. *J Hazard Mater.* 412: 125219. <https://doi.org/10.1016/j.jhazmat.2021.125219>
- Lednický J et al. 2016. Highly efficient collection of infectious pandemic influenza h1n1 virus (2009) through laminar-flow water based condensation. *Aerosol Sci Technol.* 50(7):i–iv. <https://doi.org/10.1080/02786826.2016.1179254>
- Lee D, Jang J, Jang J. 2022. Rapid detection of airborne coronaviruses using carbon nanotubes-coated paper working electrodes. In *The 26th International Conference on Miniaturized Systems for Chemistry and Life Sciences.*
- Lee D, Jang J, Jang J. 2023. Sensitive and highly rapid electrochemical measurement of airborne coronaviruses through condensation-based direct impaction onto carbon nanotube-coated porous paper working electrodes. *J Hazard Mater.* 458:131972. <https://doi.org/10.1016/j.jhazmat.2023.131972>
- Lee J, Park C, Jang J. 2024. Improved measurement of airborne viruses using a two-stage highly virus-enriching electrostatic particle concentrator with electric-field-enhancing wire electrodes. *J Hazard Mater.* 479:135747. <https://doi.org/10.1016/j.jhazmat.2024.135747>
- Li J et al. 2018. Comparing the performance of 3 bioaerosol samplers for influenza virus. *J Aerosol Sci.* 115:133–145. <https://doi.org/10.1016/j.jaerosci.2017.08.007>
- Memish ZA et al. 2014. Environmental sampling for respiratory pathogens in jeddah airport during the 2013 hajj season. *Am J Infect Control.* 42(12):1266–1269. <https://doi.org/10.1016/j.ajic.2014.07.027>
- Nguyen TT et al. 2017. Bioaerosol sampling in clinical settings: a promising, noninvasive approach for detecting respiratory viruses. In *Open forum infectious diseases.* Oxford University Press US.
- Oh S et al. 2010. Development and evaluation of a novel bioaerosol amplification unit (BAU) for improved viral aerosol collection. *J Aerosol Sci.* 41(9):889–894. <https://doi.org/10.1016/j.jaerosci.2010.06.002>
- Pan M et al. 2016. Efficient collection of viable virus aerosol through laminar-flow, water-based condensational particle growth. *J Appl Microbiol.* 120(3):805–815. <https://doi.org/10.1111/jam.13051>
- Pan M et al. 2017. Collection of viable aerosolized influenza virus and other respiratory viruses in a student health care center through water-based condensation growth. *mSphere.* 2(5):10–1128. <https://doi.org/10.1128/msphere.00251-17>
- Pan M, Lednický JA, Wu CY. 2019. Collection, particle sizing and detection of airborne viruses. *J Appl Microbiol.* 127(6):1596–1611. <https://doi.org/10.1111/jam.14278>
- Park C, Jang J, Jang J. 2025. Airborne influenza virus surveillance platform using paper-based immunosensors and a growth-based virus aerosol concentrator. *Environ Sci Technol.* 59(13): 6502–6511. <https://doi.org/10.1021/acs.est.4c14065>
- Riemenschneider L et al. 2010. Characterization of reaerosolization from impingers in an effort to improve airborne virus sampling. *J Appl Microbiol.* 108(1):315–324. <https://doi.org/10.1111/j.1365-2672.2009.04425.x>
- Shiu EYC et al. 2020. Frequent recovery of influenza a but not influenza b virus RNA in aerosols in pediatric patient rooms. *Indoor Air.* 30(5):805–815. <https://doi.org/10.1111/ina.12669>

- Sousan S, Fan M, Outlaw K, Williams S, Roper RL. 2022. Sars-cov-2 detection in air samples from inside heating, ventilation, and air conditioning (HVAC) systems-covid surveillance in student dorms. *Am J Infect Control*. 50(3):330–335. <https://doi.org/10.1016/j.ajic.2021.10.009>
- Turgeon N, Toulouse M-J, Martel B, Moineau S, Duchaine C. 2014. Comparison of five bacteriophages as models for viral aerosol studies. *Appl Environ Microbiol*. 80(14):4242–4250. <https://doi.org/10.1128/AEM.00767-14>
- Vass WB et al. 2022. Viable sars-cov-2 delta variant detected in aerosols in a residential setting with a self-isolating college student with covid-19. *J Aerosol Sci*. 165:106038. <https://doi.org/10.1016/j.jaerosci.2022.106038>
- Vass WB et al. 2023. Detection and isolation of infectious SARS-COV-2 omicron subvariants collected from residential settings. *Aerosol Sci Technol*. 57(11):1142–1153. <https://doi.org/10.1080/02786826.2023.2251537>
- Vass WB et al. 2024. Concentrating viable airborne pathogens using a virtual impactor with a compact water-based condensation air sampler. *Aerosol Sci Technol*. 58(10):1114–1128. <https://doi.org/10.1080/02786826.2024.2380096>
- Verreault D, Moineau S, Duchaine C. 2008. Methods for sampling of airborne viruses. *Microbiol Mol Biol Rev*. 72(3):413–444. <https://doi.org/10.1128/mnbr.00002-08>
- Vives JT et al. 2022. SARS-COV-2 detection in bioaerosols using a liquid impinger collector and DDPCR. *Indoor Air*. 32:e13002. <https://doi.org/10.1111/ina.13002>
- Wang CC et al. 2021. Airborne transmission of respiratory viruses. *Science*. 373(6558):eabd9149. <https://doi.org/10.1126/science.abd9149>
- Wei Z, Rosario RC, Montoya LD. 2010. Collection efficiency of a midjet impinger for nanoparticles in the range of 3–100 nm. *Atmos Environ*. 44(6):872–876. <https://doi.org/10.1016/j.atmosenv.2009.11.037>
- Willeke K, Lin X, Grinshpun SA. 1998. Improved aerosol collection by combined impaction and centrifugal motion. *Aerosol Sci Technol*. 28(5):439–456. <https://doi.org/10.1080/02786829808965536>
- Woo M-H, Grippin A, Wu C-Y, Baney RH. 2012. Use of dialdehyde starch treated filters for protection against airborne viruses. *J Aerosol Sci*. 46:77–82. <https://doi.org/10.1016/j.jaerosci.2011.09.006>
- Yu K-P, Chen Y-P, Gong J-Y, Chen Y-C, Cheng C-C. 2016. Improving the collection efficiency of the liquid impinger for ultrafine particles and viral aerosols by applying granular bed filtration. *J Aerosol Sci*. 101:133–143. <https://doi.org/10.1016/j.jaerosci.2016.08.002>
- Zheng Y, Yao M. 2017. Liquid impinger biosampler's performance for size-resolved viable bioaerosol particles. *J Aerosol Sci*. 106:34–42. <https://doi.org/10.1016/j.jaerosci.2017.01.003>
- Zuo Z et al. 2014. Survival of airborne ms2 bacteriophage generated from human saliva, artificial saliva, and cell culture medium. *Appl Environ Microbiol*. 80(9):2796–2803. <https://doi.org/10.1128/AEM.00056-14>